ARTICLES

Many-body calculation of the magnetic, optical, and charge-transfer spectra of solid oxygen in the α and β phases

Antônio J. R. da Silva* and L. M. Falicov†

Department of Physics, University of California at Berkeley and Materials Sciences Division, Lawrence Berkeley Laboratory, University of California, Berkeley, California 94720

(Received 29 August 1994)

The electronic spectra of α and β solid O_2 were calculated in a full many-body approach for a cluster consisting of four O_2 molecules with periodic-boundary conditions. By including only the partially occupied π orbitals (16 spin orbitals, 8 electrons) the basis set consists of 12 870 many-electron states. The resulting spectra contains three basic types of excitations at very different energy ranges: (a) 81 states corresponding to the ground state and magnetic excitations (magnons) within 100 meV; (b) 1215 states of neutral molecular excitations (excitons) with energies from about 1 to 8 eV; and (c) 11 574 charge-transfer states with excitation energies up to 60 eV. Analysis of the properties of the ground states in both α and β solid O_2 has been carried out. The lowest many-body states, those that correspond to neutral, unexcited molecules, describe accurately the magnetic excitations of both solids. The two phases have very different spectra resulting, even at very low temperatures, in a sizeable difference in the (magnetic) entropy. The calculated entropy difference at the observed α-β phase transition temperature agrees surprisingly well with the experimentally measured heat of transformation.

I. INTRODUCTION

In the present work, a full many-body calculation for the electronic structure of molecular-solids α-O_2 and β-O_2 is performed. A very good description of the low-lying electronic excitations (in the meV range), which are related to the magnetic properties of solid oxygen, is obtained. As a result it was possible to establish the importance of the magnetic excitations in the phase transition between the two lowest-temperature phases of solid oxygen, the so called α-β phase transition. The present calculation also describes very well optical excitations in the solid, which resemble, in their gross features, excitations in gaseous molecular oxygen. Before the properties of the solid are discussed, a brief review of the oxygen molecule and its properties is in order.[1,2]

Oxygen is a homonuclear diatomic molecule with two unpaired electrons in the π_g valence molecular orbitals derived from the $2p$ shell of each oxygen atom. The ground-state molecular-orbital configuration of the oxygen molecule is[1,2]

$$(1\sigma_g^+)^2(1\sigma_u^+)^2(2\sigma_g^+)^2(2\sigma_u^+)^2(1\pi_u)^4(3\sigma_g^+)^2(1\pi_g)^2 \ . \quad (1)$$

Three molecular states may arise from the open-shell $(\pi_g)^2$ configuration, $^1\Sigma_g^+$ ($S = 0, \Lambda = 0$), $^1\Delta_g$ ($S = 0, \Lambda = 2$), and $^3\Sigma_g^-$ ($S = 1, \Lambda = 0$), which are a result of the six possible ways the two electrons can be placed in the π_g orbitals. The degeneracy of each state is given by $(2S+1)$ for $\Lambda = 0$ and by $2(2S+1)$ for $\Lambda \neq 0$, where S is the total spin quantum number and Λ is the component of the resultant electronic orbital angular momentum parallel to the internuclear axis. The subscripts g and u in the spectroscopy notation for the molecular states denote even and odd states under inversion through the center of the molecule, and the superscripts + and − for the Σ states refer to even and odd states with respect to reflection in any plane containing the internuclear axis.

These molecular states would be degenerate were it not for the Coulomb interaction between the electrons. By Hund's rules, the $^3\Sigma_g^-$ state has the lowest energy, the $^1\Delta_g$ state, next higher, and the $^1\Sigma_g^+$, the highest energy. Therefore, oxygen is a paramagnetic molecule with a spin-triplet ground state. In the low-pressure gas phase, transitions from the ground state $^3\Sigma_g^-$ to the upper states $^1\Delta_g$ and $^1\Sigma_g^+$ account for the entire absorption around the visible region of the spectrum, with the following assignment:

$$\text{(a)} \quad {}^3\Sigma_g^- \Longrightarrow {}^1\Delta_g \quad (7882\ \text{cm}^{-1}) \ ,$$
$$\text{(b)} \quad {}^3\Sigma_g^- \Longrightarrow {}^1\Sigma_g^+ \quad (13\,120\ \text{cm}^{-1}) \ .$$

These transitions are weak (they are electric-dipole forbidden) and have been interpreted as magnetic dipole transitions.[2]

In solid oxygen, as well as the liquid phase and compressed gaseous oxygen, the intensity of these transitions increases significantly.[3,4] In addition, three new absorption bands appear in the visible and near ultraviolet region of the spectrum, a region where there are no transitions in molecular oxygen. These bands are assigned[4,5] to simultaneous excitations of a pair of oxygen molecules as follows:

$$\text{(c)} \quad ({}^3\Sigma_g^-)({}^3\Sigma_g^-) \Longrightarrow ({}^1\Delta_g)({}^1\Delta_g) \quad (16\,800\ \text{cm}^{-1}) \ ,$$
$$\text{(d)} \quad ({}^3\Sigma_g^-)({}^3\Sigma_g^-) \Longrightarrow ({}^1\Delta_g)({}^1\Sigma_g^+) \quad (21\,000\ \text{cm}^{-1}) \ ,$$
$$\text{(e)} \quad ({}^3\Sigma_g^-)({}^3\Sigma_g^-) \Longrightarrow ({}^1\Sigma_g^+)({}^1\Sigma_g^+) \quad (27\,700\ \text{cm}^{-1}) \ .$$

0163-1829/95/52(4)/2325(11)/$06.00

All these single [(a) and (b) above] and double [(c), (d), and (e) above] intramolecular electronic excitations generate bands in the crystals. The solids have typical properties characteristic of molecular solids, such as side bands and Frenkel excitons.[3,4,6–11]

In the absence of external probes and at low temperatures, all oxygen molecules in the solid are in their electronic ground state $^3\Sigma_g^-$. In this case, the low-energy excitations (meV range) correspond to lattice excitations, such as acoustic vibrations (phonons) and libration of the molecules as a whole (librons), which are common to all diatomic molecular solids.[12–14] In addition, there are magnetic excitations (magnons) that are not present in other molecular crystals.[6,7,15–18] These magnetic excitations are a result of the triplet^2 ($S = 1$) ground state of the oxygen molecule.

The lowest-temperature phase (at atmospheric pressure) of oxygen is the solid α-O_2. It is stable[19] below 23.9 K, has a monoclinic structure, space group $C2/m$, and one molecule per chemical primitive unit cell[20] (Fig. 1). The molecules in α oxygen are orientationally ordered, with the molecular axis perpendicular to the a-b plane. These planes have center-rectangular symmetry and each molecule has four-nearest neighbors, at a distance of 3.20 Å, and two second-nearest neighbors, at 3.43 Å. The third-nearest neighbors of each molecule, four in number and at an intermolecular separation of 4.19 Å, are in adjacent planes.[20,21] Monoclinic α-O_2 is the only elemental solid that is known to be both insulating and antiferromagnetic. It is known that all spins are aligned along the monoclinic axis $\pm\mathbf{b}$, with all nearest neighbors in an antiparallel arrangement to each other.[20,22–25]

β oxygen, which is the stable phase of oxygen[19,26] from 23.9 K to 43.8 K, is rhombohedral, with space group $R3\overline{m}$, and also has one molecule per primitive cell. The molecules are also orientationally ordered. They are packed in layers with their axis perpendicular to the layer planes (the equivalent of the a-b planes in α-O_2, see Fig. 2). These layers form a hexagonal lattice, with a triangular arrangement of the molecules in each plane. This spatial arrangement has the consequence that β-O_2 cannot be a classical antiferromagnet: frustration

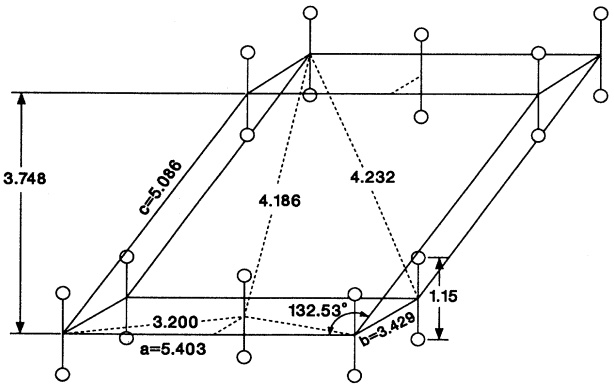

FIG. 1. Crystal structure of molecular solid α-O_2. Internuclear axes are drawn normal to the a-b planes. All lattice constants are in Å.

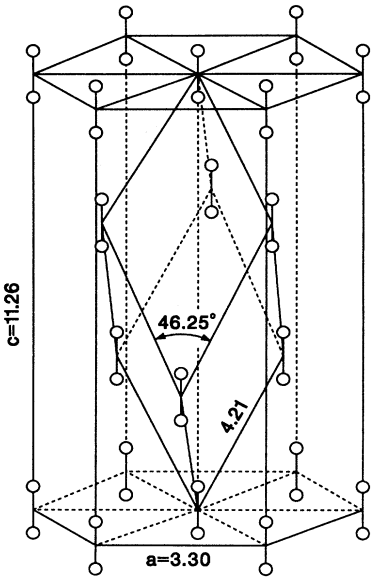

FIG. 2. Crystal structure of molecular solid β-O_2. Internuclear axes are drawn normal to the hexagonal planes. These planes are the equivalents to the a-b planes in α-O_2. All lattice constants are in Å.

prevents all nearest neighbors from aligning themselves in an antiparallel configuration. Although susceptibility measurements[22,27] have indicated a behavior characteristic of antiferromagnets, no long-range order is observed in neutron scattering experiments. There is, however, evidence of short-range order.[23–25,28,29]

Different models[30–34] have been proposed to explain the magnetic structure of β-O_2. They normally use an effective Heisenberg spin Hamiltonian to describe the magnetic interactions in solid oxygen. A recent[29] polarized neutron scattering experiment suggests that the molecular spins in β-O_2 would form a two-dimensional, short-range-order helix, with the axis perpendicular to the threefold axis, an angle close to 140° between neighboring molecular axes, and with a correlation length of 5 Å.

At the temperature of 23.9 K, there is a phase transition from α-O_2 to β-O_2. The α-β phase transition in itself has been a subject of great interest.[25,35–40] Although the order of the transition has been questioned in the past,[41–43] there is a consensus[19,21,39,40,44] that the α-β phase transition is, thermodynamically, of first order. This point of view is strongly supported by the discontinuous behavior of the crystal parameters at the phase transition.[16,39,40]

The transition involves a very small volume change; Roder[19] suggests a value of $\Delta V = 0.13 \pm 0.11$ cm^3/mol and the measurements of Krupskiĭ *et al.*[16] give $\Delta V = 0.04 \pm 0.08$ cm^3/mol. Such a small volume change is also obtained in Monte Carlo calculations.[40] The structures of α and β oxygen are very similar.[21,44,45] The hexagonal planes in β-O_2 can be obtained from the center-rectangular planes of α-O_2 by a very small distortion. It has been shown theoretically[45,46] that magnetic interac-

tions are responsible for the stability of the α phase at low temperatures. It has been proposed[17,25,40,46] that the structural distortions from the geometrically most favorable β-O_2 phase to the α-O_2 phase take place in order to minimize the magnetic energy. Although this is true at temperatures well below the transition temperature, the contribution of the magnetic entropy to the phase transition has not been clearly elucidated yet.[47] Therefore, even though the importance of the different magnetic structures of α-O_2 and β-O_2 for the α-β phase transition is a well established fact, further studies are necessary to understand the transition mechanism. The present calculation gives a clear answer to this problem.[48]

Both α and β oxygen are insulators. Band theory yields for both phases a half-filled band derived from the $2p$-π antibonding orbitals, i.e., a metal, which is in contradiction with the experimental results. Solid O_2 is therefore a prototypical Mott insulator.[49]

From the presentation above it can be seen that any theoretical treatment of molecular solid O_2 requires, from the start, the inclusion of the strong electron-electron correlations. Solid oxygen can actually be viewed as a set of weakly interacting molecules with strong intramolecular correlations. The dominant (but weak) intermolecular electronic interactions are short ranged. This fact makes solid oxygen an ideal candidate in which to study electronic spectra by the so-called small-cluster method.[50] The method treats one-electron and many-body effects on the same footing, but restricts itself to a "small crystal" (a few unit cells with periodic-boundary conditions) or, equivalently, samples only a few, symmetry-related, select points in reciprocal space.

In the present work, an exact diagonalization of the many-electron Hamiltonian for a small cluster of four O_2 molecules is performed. The molecules are in a planar arrangement (the a-b plane) with periodic-boundary conditions (see Fig. 3). The use of the periodic-small-cluster approximation in treating strong correlated materials is well established.[50] As treated here, the method determines accurately the full many-body states of a periodic cluster of four molecules, including excited electronic

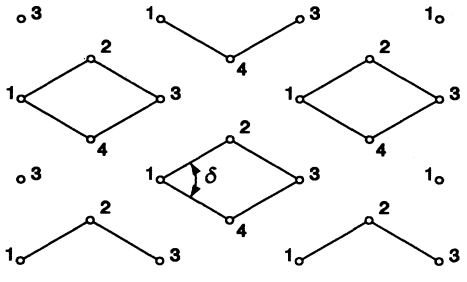

FIG. 3. One of the planes perpendicular to the molecular axis in α-O_2 or β-O_2. If the angle δ is equal to $\delta = 64.4°$ the plane has center-rectangular symmetry and corresponds to one of the a-b planes of molecular solid α-O_2. On the other hand, if $\delta = 60°$, the plane has hexagonal symmetry and corresponds to one of the planes of molecular solid β-O_2. The periodic small cluster used in the calculations is shown in detail, and contains four sites (molecules) labeled 1, 2, 3, and 4.

states of neutral O_2, as well as charge-transfer states. Magnetic interactions and excitations within the present model follow naturally from the many-body electronic structure calculation, and do not have to be introduced *a posteriori*. Therefore, this method should provide a good description, qualitative and quantitative, of the magnetic excitations in α and β oxygen.

The paper is organized in the following way. The next section derives in detail the many-body Hamiltonian used in the calculation. The resulting spectra and ground-state properties are analyzed in Sec. III, and the conclusions are presented in the last section.

II. HAMILTONIAN AND METHOD OF SOLUTION

As mentioned before, solid oxygen is an ideal candidate for the application of the small-cluster formalism. The cluster used in the present work contains four oxygen molecules, all in a single plane perpendicular to the molecular axis (see Fig. 1 and Fig. 2). This cluster is shown in detail in Fig. 3. Interplane exchange interactions, which are much weaker,[23,25] are completely neglected. By imposing periodic-boundary conditions, this cluster choice is equivalent to a sampling of four points in the Brillouin zone (reciprocal space) of solid oxygen.[50] Within the cluster, molecules are labeled from 1 to 4. In α oxygen each molecule, say that labeled 1, has (with periodic-boundary conditions included) two each of the molecules 2 and 4 as nearest neighbors, and two of the molecules 3 as second-nearest neighbors. In β oxygen the six-nearest neighbors to molecule 1 are two each of the other molecules, 2, 3, and 4 (see Fig. 3).

Only the valence electrons of the oxygen molecules have been considered explicitly. There are two per molecule, and a total of eight in the cluster. The Hilbert-space basis vectors consist of a set of mutually orthogonal Löwdin spin orbitals[51] of the O_2 molecule, two of each spin on each molecule. When the molecules are far apart, these are the real x and y orbitals corresponding to π_g^- symmetry and derived from the atomic-oxygen $2p$ states. With this set of one-particle functions—a total of sixteen spin orbitals—and the eight electrons in the cluster, a total of 12 870 many-particle states can be obtained. These states may then be used to construct the Hamiltonian matrix.

The Hamiltonian can be best written using the second-quantization formalism. Attached to each Löwdin spin orbital there is a creation (destruction) operator $a^\dagger_{i\mu\sigma}$ ($a_{i\mu\sigma}$), where i stands for the molecular site (location of the O_2 molecules, ranging from 1 to 4 in the present calculation), μ for the spatial π orbital (x or y), and σ for the spin ($\uparrow$ or $\downarrow$). The Hamiltonian contains one- and two-particle terms:

$$H = \sum_{ij}\sum_{\mu\nu}\sum_{\sigma} t_{ij}^{\mu\nu} a^\dagger_{i\mu\sigma} a_{j\nu\sigma} + \frac{1}{2}\sum_{ijkl}\sum_{\mu\nu\epsilon\lambda}\sum_{\sigma\sigma'} U_{ijkl}^{\mu\nu\epsilon\lambda} a^\dagger_{i\mu\sigma} a^\dagger_{j\nu\sigma'} a_{k\epsilon\sigma'} a_{l\lambda\sigma} , \quad (2)$$

where $t_{ij}^{\mu\nu}$ and $U_{ijkl}^{\mu\nu\epsilon\lambda}$ are the one- and two-particle matrix elements. This Hamiltonian can be rewritten as[9]

$$H = \sum_i H_i + H_{\rm int} \ , \tag{3}$$

where $\sum_i H_i$ is the Hamiltonian of infinitely separated, noninteracting molecules, and $H_{\rm int}$ accounts for those contributions involving more than one molecule at a time. Following Bhandari and Falicov,[9] the Hamiltonian for one single O_2 molecule, H_i, is

$$\begin{aligned} H_i = \alpha \sum_\sigma [n_{i\sigma} + \overline{n}_{i\sigma}] + U[n_{i\uparrow}n_{i\downarrow} + \overline{n}_{i\uparrow}\overline{n}_{i\downarrow}] + (U-2W)[n_{i\uparrow}\overline{n}_{i\downarrow} + n_{i\downarrow}\overline{n}_{i\uparrow}] \\ +(U-3W)[n_{i\uparrow}\overline{n}_{i\uparrow} + n_{i\downarrow}\overline{n}_{i\downarrow}] + W[a^\dagger_{ix\uparrow}a_{iy\uparrow}a^\dagger_{ix\downarrow}a_{iy\downarrow} \\ +a^\dagger_{ix\uparrow}a_{iy\uparrow}a^\dagger_{iy\downarrow}a_{ix\downarrow} + a^\dagger_{iy\uparrow}a_{ix\uparrow}a^\dagger_{ix\downarrow}a_{iy\downarrow} + a^\dagger_{iy\uparrow}a_{ix\uparrow}a^\dagger_{iy\downarrow}a_{ix\downarrow}] \ , \end{aligned} \tag{4}$$

where

$$n_{i\sigma} = a^\dagger_{ix\sigma}a_{ix\sigma} \ , \quad \overline{n}_{i\sigma} = a^\dagger_{iy\sigma}a_{iy\sigma} \ . \tag{5}$$

The parameter α is the one-electron energy corresponding to each of the π orbitals and U and W are the Coulomb and exchange integrals, respectively, given by

$$U = \int \pi^2_{ix}(\mathbf{r}_1)v(\mathbf{r}_1,\mathbf{r}_2)\pi^2_{ix}(\mathbf{r}_2)d^3r_1d^3r_2 \tag{6}$$

and

$$\begin{aligned} W = \int \pi_{ix}(\mathbf{r}_1)\pi_{iy}(\mathbf{r}_2)v(\mathbf{r}_1,\mathbf{r}_2) \\ \times\pi_{ix}(\mathbf{r}_2)\pi_{iy}(\mathbf{r}_1)d^3r_1d^3r_2 \ . \end{aligned} \tag{7}$$

In (6) and (7), $v(\mathbf{r}_1,\mathbf{r}_2)$ is the screened Coulomb interaction between two electrons. All the parameters for the on-site Hamiltonian — α, U, W — were fitted, as done by Bhandari and Falicov,[9] using experimental data for the ionization potential, electron affinity, and optical absorption frequencies of the oxygen molecule. The obtained numerical values are

$$\alpha = -22.75 \text{ eV}, \quad U = 11.60 \text{ eV}, \quad \text{and} \quad W = 0.45 \text{ eV} \ . \tag{8}$$

When the intermolecular interaction Hamiltonian $H_{\rm int}$ is included (by bringing the molecules closer together), the Löwdin spin orbitals change their structure. It is assumed that this change, for the separations involved, does not affect the single-molecule parameters significantly, and that the values from Eq. (8) are valid for solid O_2. The interaction Hamiltonian, $H_{\rm int}$, can be separated into one- and two-electron terms,

$$H_{\rm int} = H^{1e}_{\rm int} + H^{2e}_{\rm int} \ . \tag{9}$$

The one-electron part of the interaction Hamiltonian, $H^{1e}_{\rm int}$, contains both hopping and crystal-field terms, and can be written as

$$H^{1e}_{\rm int} = \sum_{i,\sigma}(\gamma_x n_{i\sigma} + \gamma_y \overline{n}_{i\sigma}) + 2\sum_{i<j} H^{\rm hop}_{ij} \ . \tag{10}$$

In the above equation γ_x and γ_y are the crystal-field integrals,

$$\gamma_\mu = \int \pi^2_{i\mu}(\mathbf{r}) \sum_{j\neq i} u(\mathbf{r}-\mathbf{R}_j)d^3r \ , \tag{11}$$

where $u(\mathbf{r}-\mathbf{R}_j)$ is the screened one-electron potential seen by an electron and arising from the molecule centered at position $\mathbf{R}_j$, and μ can be x or y. In Eq. (10), $H^{\rm hop}_{ij}$ represents the hopping between sites i and j. The factor of two in (10) is a result of the periodic boundary conditions. The hopping Hamiltonian $H^{\rm hop}_{ij}$ is written as

$$\begin{aligned} H^{\rm hop}_{ij} = \sum_\sigma [t^{xx}_{ij}(a^\dagger_{ix\sigma}a_{jx\sigma} + a^\dagger_{jx\sigma}a_{ix\sigma}) \\ +t^{xy}_{ij}(a^\dagger_{ix\sigma}a_{jy\sigma} + a^\dagger_{jy\sigma}a_{ix\sigma} \\ +a^\dagger_{iy\sigma}a_{jx\sigma} + a^\dagger_{jx\sigma}a_{iy\sigma}) \\ +t^{yy}_{ij}(a^\dagger_{iy\sigma}a_{jy\sigma} + a^\dagger_{jy\sigma}a_{iy\sigma})] \ . \end{aligned} \tag{12}$$

If three- and four-center integrals are neglected, the hopping matrices can be written as

$$t^{\mu\nu}_{ij} = \int \pi_{i\mu}(\mathbf{r})u(\mathbf{r}-\mathbf{R}_i)\pi_{j\nu}(\mathbf{r})d^3r \ , \tag{13}$$

where μ and ν stand for x or y.

Finally, the two-electron term in the interaction Hamiltonian $H^{2e}_{\rm int}$ is

$$\begin{aligned} H^{2e}_{\rm int} = 2\sum_{i<j}\sum_{\sigma,\sigma'}[U^{xxxx}_{ij}(n_{i\sigma}n_{j\sigma'}) + U^{yyyy}_{ij}(\overline{n}_{i\sigma}\overline{n}_{j\sigma'}) + U^{xyyx}_{ij}(n_{i\sigma}\overline{n}_{j\sigma'} + \overline{n}_{i\sigma}n_{j\sigma'}) \\ +U^{xxyy}_{ij}(a^\dagger_{ix\sigma}a_{iy\sigma}a^\dagger_{jx\sigma'}a_{jy\sigma'} + a^\dagger_{ix\sigma}a_{iy\sigma}a^\dagger_{jy\sigma'}a_{jx\sigma'} \\ +a^\dagger_{iy\sigma}a_{ix\sigma}a^\dagger_{jx\sigma'}a_{jy\sigma'} + a^\dagger_{iy\sigma}a_{ix\sigma}a^\dagger_{jy\sigma'}a_{jx\sigma'}) \\ +U^{xyyy}_{ij}(a^\dagger_{ix\sigma}a_{iy\sigma}\overline{n}_{j\sigma'} + \overline{n}_{i\sigma}a^\dagger_{jx\sigma'}a_{jy\sigma'} + a^\dagger_{iy\sigma}a_{ix\sigma}\overline{n}_{j\sigma'} + \overline{n}_{i\sigma}a^\dagger_{jy\sigma'}a_{jx\sigma'}) \\ +U^{xxxy}_{ij}(a^\dagger_{ix\sigma}a_{iy\sigma}n_{j\sigma'} + n_{i\sigma}a^\dagger_{jx\sigma'}a_{jy\sigma'} + a^\dagger_{iy\sigma}a_{ix\sigma}n_{j\sigma'} + n_{i\sigma}a^\dagger_{jy\sigma'}a_{jx\sigma'})] \ . \end{aligned} \tag{14}$$

The Coulomb and exchange integrals $U_{ij}^{\mu\nu\epsilon\lambda}$ are given by

$$U_{ij}^{\mu\nu\epsilon\lambda} = \int \pi_{i\mu}(\mathbf{r}_1)\pi_{j\nu}(\mathbf{r}_2)v(\mathbf{r}_1,\mathbf{r}_2) \times\pi_{j\epsilon}(\mathbf{r}_2)\pi_{i\lambda}(\mathbf{r}_1)d^3r_1d^3r_2 \quad . \tag{15}$$

Terms neglected in Eq. (14) involve overlap between orbitals on different molecules. These are expected to be small.

As can be noted from Eqs. (11), (13), and (15), all parameters in $H_{\rm int}$ involve only two molecules or a sum of terms each of which depends only on two molecules at a time. To calculate the parameters it is convenient to rotate, for each pair, the Löwdin orbitals (change of basis) so that they are either in the plane of the two molecules, or perpendicular to that plane (see Fig. 4). The orbital oriented along the molecular plane is called π_ξ and the one oriented in the direction perpendicular to the plane is denoted π_η. For a given site i, the orbitals π_{ix} and π_{iy} can be written as a function of the new orbitals $\pi_{i\xi}$ and $\pi_{i\eta}$,

$$\begin{aligned} \pi_{ix} &= \pi_{i\xi}\cos\theta + \pi_{i\eta}\sin\theta \quad , \\ \pi_{iy} &= \pi_{i\xi}\sin\theta - \pi_{i\eta}\cos\theta \quad , \end{aligned} \tag{16}$$

where θ is the angle between the intermolecular axis and the x axis, as shown in Fig. 5.

With the above equations, all parameters in $H_{\rm int}$ can be rewritten as functions of the new orbitals π_ξ and π_η and the angle θ. The dependence on the new orbitals appears through the following integrals:[9]

$$\begin{aligned} \gamma_\beta(R) &= \int \pi_{i\beta}^2(\mathbf{r})u(\mathbf{r}-\mathbf{R}_j)d^3r \quad , \\ V_\beta(R) &= \int \pi_{i\beta}(\mathbf{r})u(\mathbf{r}-\mathbf{R}_i)\pi_{j\beta}(\mathbf{r})d^3r \quad , \end{aligned}$$

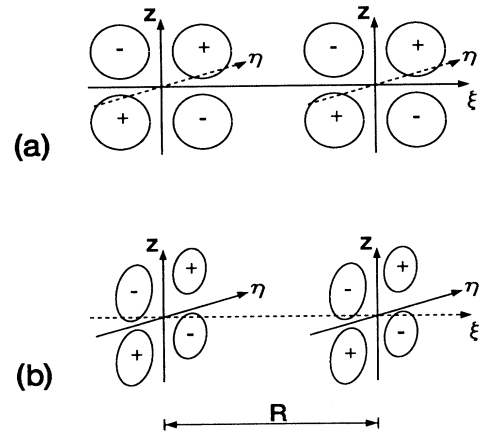

FIG. 4. Orientation of the orbitals (a) π_ξ and (b) π_η. The molecules have their own axes along $\hat{z}$, always perpendicular to the line joining the two molecular centers, separated by the distance R. The orbital π_ξ is in the plane determined by the molecular and the intermolecular axes; the orbital π_η is in a plane perpendicular to the intermolecular axis.

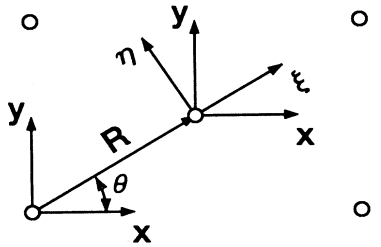

FIG. 5. Relative orientation between the (xy) and $(\xi\eta)$ axes for a pair of oxygen molecules. The O_2 molecules are along $\hat{z}$ axes, perpendicular to the figure, and their positions are marked by the circles. The $(\xi\eta)$ axes are rotated with respect to the (xy) axes by the angle θ, which is the angle between the intermolecular axis ξ and the x axis.

$$\begin{aligned} K_\beta(R) &= \int \pi_{i\beta}^2(\mathbf{r}_1)v(\mathbf{r}_1,\mathbf{r}_2)\pi_{j\beta}^2(\mathbf{r}_2)d^3r_1d^3r_2 \quad , \\ L(R) &= \int \pi_{i\xi}^2(\mathbf{r}_1)v(\mathbf{r}_1,\mathbf{r}_2)\pi_{j\eta}^2(\mathbf{r}_2)d^3r_1d^3r_2 \quad , \\ P(R) &= \int \pi_{i\xi}(\mathbf{r}_1)\pi_{j\xi}(\mathbf{r}_2)v(\mathbf{r}_1,\mathbf{r}_2)\pi_{j\eta}(\mathbf{r}_2) \\ &\quad \times\pi_{i\eta}(\mathbf{r}_1)d^3r_1d^3r_2 \quad , \end{aligned} \tag{17}$$

which depend only on the intermolecular separation R between the sites i and j. The indices i and j represent the neighboring molecules on which the π_ξ and π_η orbitals are located, and β stands for ξ or η. From the above integrals, $\gamma_\beta(R)$ are used to calculate the crystal-field parameters in Eq. (11), $V_\beta(R)$ to calculate the hopping integrals defined in Eq. (13), and $K_\beta(R)$, $L(R)$, and $P(R)$ to calculate the Coulomb and exchange terms in Eq. (15). A point-charge model was used to evaluate all integrals in Eq. (17), with the exception of the hopping parameters, V_ξ and V_η. Care was taken to position the charges in such a way that the experimental value of the quadrupole moment for the O_2 molecule[52] was reproduced. The values of the parameters obtained in this way are insensitive to the particular position of the point charges. For an intermolecular separation of $R = 3.20$ Å, equal to the distance between nearest neighbors in α-O_2, the resulting parameters are

$$\begin{aligned} \gamma_\xi &= -4.5 \text{ eV}, \quad \gamma_\eta = -4.2 \text{ eV} \quad , \\ K_\xi &= 2.4 \text{ eV}, \quad K_\eta = 2.0 \text{ eV} \quad , \\ L &= 2.2 \text{ eV}, \quad P = 0.0 \text{ eV} \quad . \end{aligned} \tag{18}$$

The calculated value of P is so much smaller than the other integrals that it can be taken effectively as zero within the accuracy considered. For other neighbors — both in α and β oxygen — an R-dependence $I \propto R^{-1}$ fits well the calculated values of these parameters for different intermolecular distances, where I is any one of the parameters in (18). This is expected if one notices that all these parameters are basically Coulomb interactions between localized charge densities separated by a distance R.

Because of the orientation of the orbitals, the hopping parameter V_η is much smaller than V_ξ and was neglected,

$$V_\eta(R) = 0 \quad . \tag{19}$$

The remaining matrix element, V_ξ, was determined by fitting the low-energy magnetic excitations for the α-O_2 phase. With the experimental[25,53] value $J = 4.88$ meV of the phenomenological Heisenberg interaction, the best fit was

$$V_\xi = 0.13 \text{ eV} \quad . \tag{20}$$

This value is for an intermolecular separation of $R = 3.20$ Å, equal to the distance between nearest neighbors in α-O_2. For other distances — both in α and β oxygen — an R-dependence $V_\xi \propto R^{-5}$ has been assumed.[9,25] This dependence yields $V_\xi = 0.09$ eV for the second neighbors in α-O_2 and $V_\xi = 0.11$ eV for the nearest neighbors in β-O_2.

The Hamiltonian was numerically diagonalized for the values of parameters discussed above, and for α and β oxygen. The exact diagonalization is possible through the use of group-theoretical techniques that take fully into account space and spin symmetries. The largest matrix to be diagonalized was 592 × 592. The resulting spectra are discussed below.

III. RESULTS

For each of the solid phases (α- and β-O_2) considered in this work there are, in the four-molecule cluster, 12 870 many-electron states. Eighty-one of these correspond to all O_2 molecules in their neutral ground electronic state $^3\Sigma_g^-$. They include the ground state(s) of the many-molecule system and all the magnetic excitations (i.e., various relative orientations of the molecular spins). One can picture these excitations as states where all the molecules are in the $^3\Sigma_g^-$ ground state and which differ basically in the way the molecular spins are aligned and coupled. There are additional 1215 states that correspond to all neutral O_2 molecules, but with at least one molecule in an excited state, either $^1\Delta_g$ or $^1\Sigma_g^+$. These are solid-state molecular Frenkel excitons, and among those are the single and double excitations discussed in the introduction. Finally, 11 655 states exhibit one or more units of electron-charge transfer. Calculated densities of states are shown in Figs. 6–11. Figures 6 and 9 show the full spectra of α and β oxygen, respectively. The spectra are similar; the first narrow peaks within 8 eV correspond to the molecular Frenkel excitons, which are then followed by a broadband related to the transfer of one unit of charge between sites. The sequence

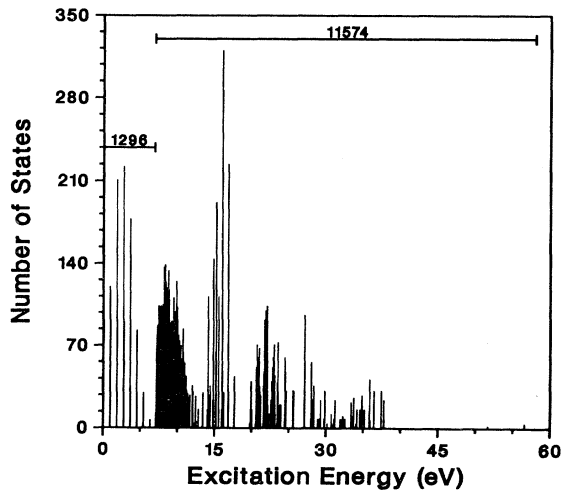

FIG. 6. Spectrum of α-O_2, including all 12 870 states. The numbers above each region of the spectrum indicate the total number of states contained in that region. All states, with the exception of the lowest 1296, are electron-charge-transfer states.

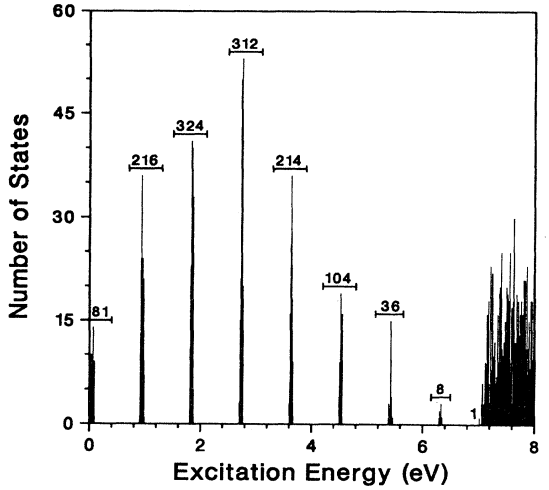

FIG. 7. Spectrum for the lowest 1296 (neutral) states of α-O_2. These states correspond to magnetic excitations and Frenkel excitons. The numbers above each band indicate the total number of states contained in that band.

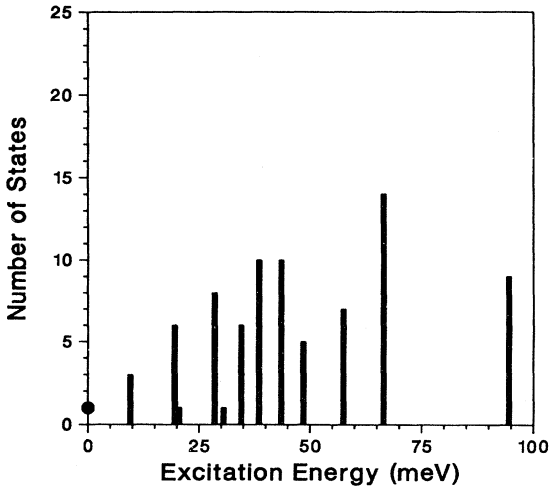

FIG. 8. Lowest 81 states (magnetic excitations) of α-O_2. The single, nondegenerate ground state is indicated by a circle at zero excitation energy.

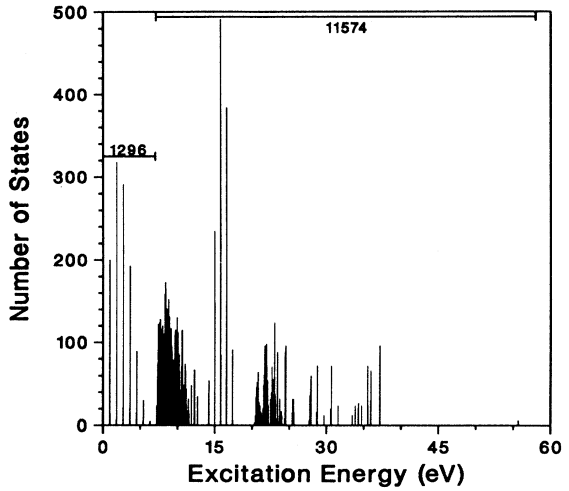

FIG. 9. Spectrum of β-O_2 including all 12 870 states. The numbers above each region of the spectrum indicate the total number of states contained in that region. All states, with the exception of the lowest 1296, are electron-charge-transfer states.

of sharp peaks and narrow bands that start from about 13 eV contain all the states with more than one unit of charge transferred between molecules. If this spectrum is compared with a previous calculation,[54] which used the same method but neglected all intersite Hamiltonian parameters except the hopping V_ξ, one can see that the main effect of the intersite Coulomb terms is to lower the energy of the charge-transfer states, a result of the Madelung interaction between charged molecules.[55]

Figures 7 and 10 show amplified views of the 1296 lowest states (neutral molecules) of α and β oxygen, respectively, together with the first few charge-transfer levels. It is to be noticed that for four molecules the highest-

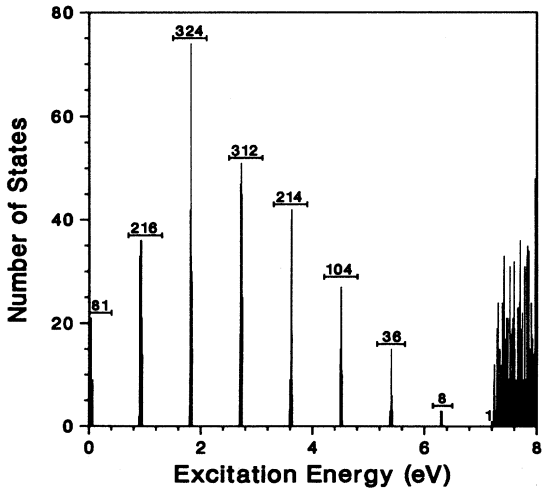

FIG. 10. Spectrum of the lowest 1296 (neutral) states of β-O_2, corresponding to magnetic excitations and Frenkel excitons. The numbers above each band indicate the total number of states contained in that band.

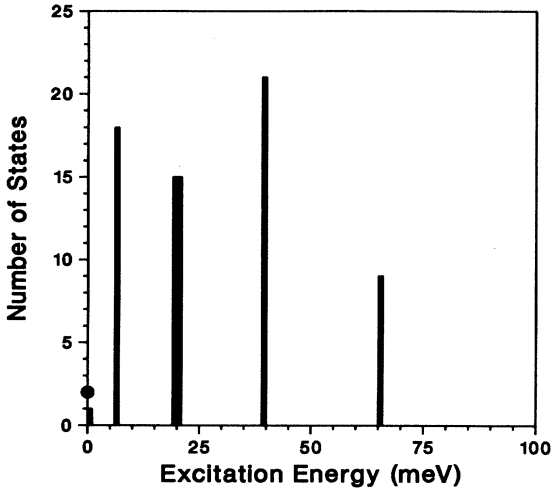

FIG. 11. Lowest 81 states (magnetic excitations) of β-O_2. Note that the ground state is doubly degenerate — circle for two states at zero excitation energy — and that there is a singlet excited state at very low energy: 0.8 meV.

energy state among these 1296 is very close to the bottom of the single charge-transfer band. Again, the overall shape of the spectrum is very similar for the two phases, the main difference being a density of states that peaks at a lower energy for β-O_2. These states include optical excitations of a single molecule, as well as simultaneous excitations of various (up to four) molecules.[9]

Figures 8 and 11 show the 81 lowest states for α and β O_2, respectively. These are the states associated with only magnetic excitations. As expected, the two spectra are very different in this energy range, reflecting the dissimilar magnetic properties observed in α and β oxygen. The total-spin operator commutes with the Hamiltonian,

TABLE I. The excitation energies (ΔE) from the ground state for the lowest 81 energy eigenstates for both α and β oxygen. The value of the total spin ($S_{\rm tot}$) for each state is also shown, and N_s denotes the number of degenerate $S_{\rm tot}$ multiplets corresponding to that level. The total degeneracy of each energy level is, therefore, given by $d = N_s(2S_{\rm tot}+1)$.

α-O_2				β-O_2			
ΔE (meV)	$S_{\rm tot}$	N_s	d	ΔE (meV)	$S_{\rm tot}$	N_s	d
0.0	0	1	1	0.0	0	2	2
9.6	1	1	3	0.8	0	1	1
19.1	1	2	6	6.3	1	3	9
20.4	0	1	1	6.9	1	3	9
28.7	2	1	5	19.9	2	3	15
28.9	1	1	3	20.0	2	2	10
30.1	0	1	1	20.3	2	1	5
34.5	1	2	6	39.7	3	3	21
38.5	2	2	10	65.9	4	1	9
43.0	2	1	5				
43.9	2	1	5				
48.5	2	1	5				
57.1	3	1	7				
66.8	3	2	14				
94.5	4	1	9				

which implies that the energy eigenstates can be classified as singlets ($S_{\rm tot}=0$), triplets ($S_{\rm tot}=1$), quintets ($S_{\rm tot}=2$), septets ($S_{\rm tot}=3$), and nonets ($S_{\rm tot}=4$). Among the 81 lowest-energy states, both for α and β-O_2, there are three singlets, six triplets, six quintets, three septets, and one nonet (see Table I).

In α-O_2 the ground-state is a nondegenerate spin singlet ($S_{\rm tot}=0$), and the first-excited state is a spin triplet ($S_{\rm tot}=1$) with an excitation energy of 9.6 meV (see Fig. 8 and Table I). The spatial symmetry of the ground state corresponds to the reciprocal-space point at the center of the Brillouin zone, whereas for the first-excited state, it corresponds to a point at the Brillouin-zone boundary. These features are consistent with the interpretation that the first-excited state in α-O_2 is a spin wave or magnon.[56] Both from Fig. 8 and Table I one can see that in α-O_2 the 81 lowest-energy states are spread over a broad range (maximum excitation energy of 94.5 meV). Moreover, there is significant overlap in energy between the singlets, triplets, and quintets. For example, there are three spin triplets with lower excitation energies than the first-excited state with $S_{\rm tot}=0$.

Figure 11 shows the magnetic spectrum of β-O_2. The ground state is also a spin singlet ($S_{\rm tot}=0$), but whereas in α-O_2 it is nondegenerate, in β-O_2 it has a space-group induced twofold degeneracy. The first-excited state is also a spin singlet and it has a very small excitation energy of 0.8 meV. Moreover, both the ground and the first-excited states have spatial symmetries corresponding to the reciprocal-space point at the center of the Brillouin zone. Therefore, for the four-molecule cluster, the lowest-energy excitation in the magnetically frustrated β oxygen does not correspond to a spin-wave excitation, but most likely to a bound pair of spin waves. As can be seen from Fig. 11, the magnetic excitation spectrum of β-O_2 is narrower than that of α-O_2, with a maximum excitation energy of 65.9 meV. The states, because of the spatial hexagonal symmetry, are highly degenerate. In addition there is a monotonic correlation between energy and total spin, such that if $S_{\rm tot}(i) > S_{\rm tot}(j)$, then $\Delta E(i) > \Delta E(j)$, with no excitation-energy overlap between states of different total spin (see Table I).

A similar small-cluster calculation[57] for a Heisenberg Hamiltonian that includes first- and second-nearest neighbors exchange interactions shows that these 81 electronic low-energy states are mapped very well, both for α and β oxygen, into the excited states of an isotropic Heisenberg Hamiltonian. The most noticeable difference is that, whereas in the Heisenberg picture β-O_2 exhibits a *triply* degenerate ground state, in the full electronic calculation the ground state is only *doubly* degenerate, but with a third *very-low-energy*, almost degenerate (excited) state, as discussed above (see Fig. 11 and Table I). The resulting Heisenberg exchange parameters[53] are $J=4.8$ meV for the α-O_2 four-nearest neighbors; $J=2.3$ meV for the α-O_2 two second neighbors; and $J=3.3$ meV for the β-O_2 six-nearest neighbors.

TABLE II. Expectation values of the operators defined in the text. They are calculated using the ground-state wave function(s) from the many-body electronic structure calculation for α-O_2 and β-O_2. The results for the spin-spin correlations for the Heisenberg model calculation are also shown. For uncoupled spins $\langle S_i^2\rangle = 2$ and $\langle \mathbf{S}_i\cdot\mathbf{S}_j\rangle_{i\neq j}=0$.

	α-O_2	β-O_2
	Electronic calculation	
$\langle n\rangle$	0.99993	1.00000
$\langle\overline{n}\rangle$	1.00007	1.00000
$\delta N/N$	0.04	0.03
$\langle S_i^2\rangle$	1.991	1.994
$\langle \mathbf{S}_i\cdot\mathbf{S}_j\rangle_{\rm NN}$	-1.490	-0.665
$\langle \mathbf{S}_i\cdot\mathbf{S}_j\rangle_{\rm NNN}$	0.989	
	Heisenberg calculation	
$\langle S_i^2\rangle$	2	2
$\langle \mathbf{S}_i\cdot\mathbf{S}_j\rangle_{\rm NN}$	$-\frac{3}{2}=-1.5$	$-\frac{2}{3}=-0.667$
$\langle \mathbf{S}_i\cdot\mathbf{S}_j\rangle_{\rm NNN}$	1	

A. Ground-state properties

The spin operators for a given site i are defined as

$$S_{ix}=\frac{1}{2}[a^\dagger_{ix\downarrow}a_{ix\uparrow}+a^\dagger_{ix\uparrow}a_{ix\downarrow}+a^\dagger_{iy\downarrow}a_{iy\uparrow}+a^\dagger_{iy\uparrow}a_{iy\downarrow}]\quad,$$
$$S_{iy}=\frac{1}{2i}[-a^\dagger_{ix\downarrow}a_{ix\uparrow}+a^\dagger_{ix\uparrow}a_{ix\downarrow}-a^\dagger_{iy\downarrow}a_{iy\uparrow}+a^\dagger_{iy\uparrow}a_{iy\downarrow}]\quad,$$
$$S_{iz}=\frac{1}{2}[n_{i\uparrow}-n_{i\downarrow}+\overline{n}_{i\uparrow}-\overline{n}_{i\downarrow}]\quad. \tag{21}$$

With these expressions, the spin-spin correlations $\langle \mathbf{S}_i\cdot\mathbf{S}_j\rangle$ are calculated for the ground states of α and β O_2, and the results are reported in Table II. For β-O_2, the data actually refer to $\langle\langle \mathbf{S}_i\cdot\mathbf{S}_j\rangle\rangle$, which is the average over the two degenerate ground states. Also shown in Table II are the average site occupations for the x-like and y-like π orbitals, $\langle n\rangle=\langle n_{i\uparrow}+n_{i\downarrow}\rangle$ and $\langle\overline{n}\rangle=\langle\overline{n}_{i\uparrow}+\overline{n}_{i\downarrow}\rangle$, respectively, together with the fluctuation in the number of electrons on each site, $\delta N/N$, where $\delta N=\sqrt{\langle N^2\rangle-\langle N\rangle^2}$ and $N=n+\overline{n}$. The site i is any of the four equivalent sites in the cluster. Again, for β-O_2, reported quantities are the averages over the two degenerate ground states.

The result for $\langle S_i^2\rangle=\langle \mathbf{S}_i\cdot\mathbf{S}_i\rangle$ shows that the spin at each site is very close to $S=1$, $\langle S_i^2\rangle=2$, as expected. The small deviation from $S=1$ is a result of the fluctuations in the number of electrons on each site, which are caused by the intermolecular hopping. The size of the fluctuation is, however, very small, of the order of 4%.

The negative spin-spin correlation for nearest neighbors, $\langle \mathbf{S}_i\cdot\mathbf{S}_j\rangle_{\rm NN}$, in α-O_2 clearly shows the antiferromagnetic character of the exchange interaction between two neighboring molecules. However, the comparison of the value of $\langle \mathbf{S}_i\cdot\mathbf{S}_j\rangle_{\rm NN}$ with the same quantity evaluated for a pair of spins $S=1$ coupled in a singlet state, $\langle \mathbf{S}_i\cdot\mathbf{S}_j\rangle_{\rm singlet}=-2$, shows that nearest-neighbor molecular pairs are not fully in singlet states. The molecular-pair spins fluctuate among singlets, triplets, and quintets. Note, however, that the total spin for the four-molecule cluster in the ground state is always a singlet, with no fluctuations.

For the next-nearest neighbors in α-O_2, the positive

value of the spin-spin correlation, $\langle \mathbf{S}_i \cdot \mathbf{S}_j \rangle_{\mathrm{NNN}} = 0.989$, indicates that these molecules are very close to full ferromagnetic coupling. The comparison with the value $\langle \mathbf{S}_i \cdot \mathbf{S}_j \rangle_{\mathrm{quintet}} = 1$ for a pair of spins with $S = 1$ coupled with the maximum value of total spin shows that, although the direct coupling between the next-nearest neighbors in solid oxygen is antiferromagnetic ($J_{\mathrm{NNN}} > 0$), the resulting ground-state magnetic structure in α-O_2 has the spins of the next-nearest-neighboring molecules coupled ferromagnetically, with their maximum value and very small fluctuations. All of these values are consistent with the correlations calculated for the ground state of the Heisenberg Hamiltonian, as seen also in Table II.

For β-O_2, the same calculation displays definitely some short-range antiferromagnetic order in this system, since the negative values of $\langle \mathbf{S}_i \cdot \mathbf{S}_j \rangle_{\mathrm{NN}}$ show a tendency towards antiparallel alignment of the spins. The fluctuations are much larger than for α-O_2, as reflected by the smaller value of $\langle \mathbf{S}_i \cdot \mathbf{S}_j \rangle_{\mathrm{NN}}$. Therefore, the present calculation strongly supports the picture that β-O_2 is not a paramagnet, but a strongly correlated, frustrated antiferromagnet with low-energy excitations well described by a Heisenberg spin Hamiltonian.

B. The α-β phase transition

The spectra in Figs. 8 and 11 have been used to calculate the magnetic contributions to the entropies, $S_\alpha(T)$ and $S_\beta(T)$, associated with the low-energy magnetic excitations.[58] Here $S(T) = -k_B \sum_{i=1}^{81} P_i(T) \ln P_i(T)$, where k_B is Boltzmann's constant and $P_i(T)$ is the thermal probability of state i. It is given by $P_i(T) = \exp(-\Delta E_i/k_B T)/Z$, where ΔE_i is the excitation energy from the ground state and Z the partition function, $Z = \sum_{i=1}^{81} \exp(-\Delta E_i/k_B T)$. All sums run through the lowest 81 states, including the ground state(s). The entropy difference $\Delta S_{\beta\alpha}(T) = S_\beta(T) - S_\alpha(T)$ at the transition temperature, $T = T_{\alpha\beta} = 23.9$ K, gives the contribution of the magnetic modes to the heat of transformation. From the data of Table I and Figs. 8 and 11 one obtains $T_{\alpha\beta}\,\Delta S_{\beta\alpha} = 0.95$ meV/molecule, which agrees remarkably well with the experimental[14] value $Q_{\beta\alpha} = T_{\alpha\beta}\,\Delta S_{\beta\alpha} \simeq 0.97$ meV/molecule.

From experimental observations it is obvious that the α phase has a lower total energy, since it is the stable phase at $T = 0$. The transformation to the β phase at such a low temperature can only be driven by (i) a very small total-energy difference between the two phases, and (ii) an entropy contribution from low-lying excited modes. These modes can only be elastic (phonons and librons) or magnetic (magnons or spin waves). The contribution to the heat of transformation at 23.9 K can only thus come from the elastic and magnetic entropies.

The astounding agreement obtained above from the *magnetic entropy alone*, is probably fortuitous, but easy to understand. The small-cluster approach, used in this calculation, does not yield a good description of the long-wavelength excitation modes. It, therefore, may exaggerate the differences between the α and β magnetic entropies, and then account for a somewhat larger magnetic share that is the case in reality.

On the other hand, it is very plausible to argue that the *difference* in entropy contributions at 23.9 K from the elastic and librational modes is either negligible or very small. The structures of α-O_2 and β-O_2 are similar. The speeds of sound in both phases[14] are almost identical (1645 m/s and 590 m/s for the longitudinal and transverse speeds in the α phase at $T = 23.5$ K; 1633 m/s and 605 m/s in the β phase at $T = 24.5$ K), which should result in negligible entropy difference from the acoustic modes (phonons). The librational modes[59] (two modes at 42 cm^{-1} and 72 cm^{-1} in the α phase at $T = 20$ K; a single doubly degenerate mode at 48 cm^{-1} in β-O_2 at $T = 25$ K) yield at 23.9 K (and assuming an Einstein spectrum for the librons, an *overestimate*) a contribution of $Q_{\beta\alpha}$ (librons) $\simeq 0.17$ meV/molecule, i.e., an upper limit of only 18% of the magnetic contribution, as calculated here.

IV. CONCLUSION

The α-O_2 and β-O_2 molecular solids were studied in the periodic small-cluster approximation. The Hamiltonian included all the intramolecular correlations necessary to describe well the oxygen molecular spectra plus intermolecular interactions. The main conclusions from this calculation are as follows.

(1) Solid α-O_2 and solid β-O_2 can be well described in the first approximation by a collection of very weakly interacting O_2 molecules. The spectra of the two phases, except in the low-energy range, are very similar to each other and to the spectrum of neutral and ionized O_2 molecules.

(2) In the O_2 molecule there are exactly $N = 2$ electrons in the antibonding π orbitals, with no number fluctuations, i.e., $(\delta N/N)_{\mathrm{molecule}} = 0$. In the solids, because of the intermolecular hopping there is a fluctuation in the number of electrons in the π orbitals; it is, however, small (of the order of 4%).

(3) In solid α-O_2, because of the monoclinic symmetry, there is an anisotropy in the occupation of the x-like and y-like π orbitals; this asymmetry is also very small, of the order of 7×10^{-5} electrons.

(4) The magnetic excitations in solid α-O_2 and in solid β-O_2 can be well described by a Heisenberg-like Hamiltonian. The exchange interaction arises from virtual hopping of electrons to neighboring molecules; these values agree well with second-order perturbation calculations.[9]

(5) Solid β-O_2 is not a paramagnet, but rather a frustrated triangular-lattice antiferromagnet, with very strong spin correlations between neighboring O_2 molecules: its excitation spectrum is remarkably well described by a Heisenberg Hamiltonian with nearest-neighbor-only interactions.

(6) Although the ground states in both solid phases are spin singlets, the ground state of β-O_2 is, because of the frustration caused by the triangular-lattice symmetry, degenerate.

(7) The magnon spectra of the two phases of solid oxygen differ considerably. In α-O_2 the 81 states are spread

over a broad range, with a maximum excitation energy of 94 meV, a mean energy of 47.9 meV, and a standard deviation of 23.0 meV. On the other hand, the spin-wave excitation spectrum of β-O_2 is narrower, and the states, because of the hexagonal symmetry, are highly degenerate. It extends up to 66 meV, has a mean energy of 26.5 meV and a standard deviation of 18.6 meV. In other words, the magnetic excitations of the trigonal β phase are less energetic, and less dispersed than in the α phase.

(8) The first-excited state in α-O_2 has an energy of 9.6 meV above the ground state, is a spin triplet ($S_{\rm tot} = 1$), and can be interpreted as being a spin-wave excitation.[56] On the other hand, the first-excited state in β-O_2 has a very small excitation energy, only 0.8 meV above the ground state, and is a spin singlet ($S_{\rm tot} = 0$). This shows that this state cannot correspond to a single spin-wave excitation and that there are other magnetic low-energy excitations in the frustrated β phase that could be thought of as bound pairs of spin waves.

(9) The difference in the magnetic-excitation spectrum is, in turn, responsible for a sizeable difference in magnetic entropy at the transition temperature 23.9 K, sufficient to account for most of the heat of transformation. In other words, the α-to-β first-order transition in solid molecular oxygen is, essentially, driven exclusively by magnetic effects.

ACKNOWLEDGMENTS

This research was supported, at the Lawrence Berkeley Laboratory, by the Director, Office of Energy Research, Office of Basic Energy Sciences, Materials Sciences Division, U.S. Department of Energy, under Contract No. DE-AC03-76SF00098. A.J.R. da Silva acknowledges support from the Brazilian Conselho Nacional de Desenvolvimento Científico e Tecnológico (CNPq).

* Author to whom all correspondence should be addressed. Present address: Department of Chemistry and Biochemistry, University of California, Los Angeles, California, 90095-1569.

† Deceased.

[1] M. Weissbluth, *Atoms and Molecules* (Academic Press, San Diego, 1978).

[2] G. Herzberg, *Spectra of Diatomic Molecules* (Van Nostrand, Princeton, 1950).

[3] J. W. Ellis and D. Kneser, Z. Phys. **86**, 583 (1933).

[4] A. Landau, E. Allin, and H. L. Welsh, Spectrochim. Acta **18**, 1 (1962).

[5] A. F. Prikhot'ko, Mol. Cryst. Liq. Cryst. **57**, 189 (1980).

[6] E. J. Wachtel and R. G. Wheeler, J. Appl. Phys. **42**, 1581 (1971).

[7] Yu. B. Gaididei, V. M. Loktev, A. F. Prikhot'ko, and L. I. Shanskiĭ, Fiz. Nizk. Temp. **1**, 1365 (1975) [Sov. J. Low Temp. Phys. **1**, 653 (1975)].

[8] Y. G. Litvinenko, V. V. Eremenko, and T. I. Garber, Phys. Status Solidi **30**, 49 (1968).

[9] R. Bhandari and L. M. Falicov, J. Phys. C **6**, 479 (1973).

[10] Yu. B. Gaididei, V. M. Loktev, A. F. Prikhot'ko, and L. I. Shanskiĭ, Pis'ma Zh. Eksp. Teor. Fiz. **18**, 164 (1973) [JETP Lett. **18**, 95 (1973)].

[11] A. F. Prikhot'ko, Yu. G. Pikus, and L. I. Shanskiĭ, Pis'ma Zh. Eksp. Teor. Fiz. **32**, 312 (1980) [JETP Lett. **32**, 287 (1980)].

[12] J. D. Wright, *Molecular Crystals* (Cambridge University Press, Cambridge, 1987).

[13] C. A. English and J. A. Venables, Proc. R. Soc. London, Ser. A **340**, 57 (1974).

[14] B. I. Verkin, *Handbook of Properties of Condensed Phases of Hydrogen and Oxygen* (Hemisphere Publishing Corporation, New York, 1990).

[15] E. J. Wachtel and R. G. Wheeler, Phys. Rev. Lett. **24**, 233 (1970).

[16] I. N. Krupskiĭ, A. I. Prokhvatilov, Yu. A. Freĭman, and A. I. Érenburg, Fiz. Nizk. Temp. **5**, 271 (1979) [Sov. J. Low Temp. Phys. **5**, 130 (1979)].

[17] A. P. J. Jansen and A. van der Avoird, J. Chem. Phys. **86**, 3583 (1987).

[18] Yu. B. Gaididei and V. M. Loktev, Fiz. Tverd Tela Leningrad **16**, 3438 (1974) [Sov. Phys. Solid State **16**, 2226 (1975)].

[19] H. M. Roder, J. Phys. Chem. Ref. Data, **7**, 949 (1978).

[20] C. S. Barrett, L. Meyer, and J. Wasserman, J. Chem. Phys. **47**, 592 (1967).

[21] C. S. Barrett and L. Meyer, Phys. Rev. **160**, 694 (1967).

[22] G. C. DeFotis, Phys. Rev. B **23**, 4714 (1981).

[23] P. W. Stephens, R. J. Birgeneau, C. F. Majkrzak, and G. Shirane, Phys. Rev. B **28**, 452 (1983).

[24] R. J. Meier and R. B. Helmholdt, Phys. Rev. B **29**, 1387 (1984).

[25] P. W. Stephens and C. F. Majkrzak, Phys. Rev. B **33**, 1 (1986).

[26] D. A. Young, *Phase Diagrams of the Elements* (University of California Press, Berkeley, 1991), p. 127.

[27] H. C. Jamieson and A. C. Hollis Hallet, in *Proceedings of the 10th International Conference on Low Temperature Physics, Moscow, 1966*, edited by M.P. Malkov (Viniti Publishing Co., Moscow, 1967), Vol. 4, p. 158.

[28] M. F. Collins, Proc. Phys. Soc. **89**, 415 (1966).

[29] F. Dunstetter, V. P. Plakhti, and J. Schweizer, J. Magn. Magn. Mater. **72**, 258 (1988).

[30] V. M. Loktev, Fiz. Nizk. Temp. **5**, 295 (1979) [Sov. J. Low Temp. Phys. **5**, 142 (1979)].

[31] V. A. Slyusarev, Yu. A. Freĭman and R. P. Yankelevich, Pis'ma Zh. Eksp. Teor. Fiz. **30**, 292 (1979) [JETP Lett. **30**, 270 (1979)].

[32] V. A. Slyusarev, Yu. A. Freĭman, and R. P. Yankelevich, Fiz. Nizk. Temp. **6**, 219 (1980) [Sov. J. Low Temp. Phys. **6**, 105 (1980)].

[33] A. P. J. Jansen, Phys. Rev. B **33**, 6352 (1986).

[34] E. Rastelli, L. Reatto, and A. Tassi, J. Phys. C **19**, L589 (1986).

[35] I. A. Burakhovich, I. N. Krupskiĭ, A. I. Prokhvatilov, Yu. A. Freĭman, and A. I. Érenburg, Pis'ma Zh. Eksp. Teor. Fiz. **25**, 37 (1977) [JETP Lett. **25**, 32 (1977)].

[36] Yu. B. Gaididei and V. M. Loktev, Fiz. Nizk. Temp. **7**, 1305 (1981) [Sov. J. Low Temp. Phys. **7**, 634 (1982)].

[37] B. Kuchta, Phys. Lett. **103A**, 202 (1984).

[38] B. Kuchta, Chem. Phys. Lett. **113**, 283 (1985).

[39] B. Kuchta, T. Luty, and R. J. Meier, J. Phys. C **20**, 585 (1987).
[40] R. LeSar and R. D. Etters, Phys. Rev. B **37**, 5364 (1988).
[41] H. J. Hoge, J. Res. Natl. Bur. Stand. **44**, 321 (1950).
[42] C. H. Fagerstroem and A. C. Hollis Hallet, Ann. Acad. Sci. Fenn. **AVI210**, 210 (1966).
[43] C. H. Fagerstroem and A. C. Hollis Hallet, J. Low Temp. Phys. **1**, 3 (1969).
[44] C. S. Barrett, L. Meyer, and J. Wasserman, Phys. Rev. **163**, 851 (1967).
[45] C. A. English and J. A. Venables, Proc. R. Soc. London Ser. A **340**, 81 (1974).
[46] R. D. Etters, A. A. Helmy, and K. Kobashi, Phys. Rev. B **28**, 2166 (1983).
[47] E. Rastelli and A. Tassi, J. Phys. C **21**, 1003 (1988), using a Heisenberg spin Hamiltonian with on-site anisotropies to describe the magnetic interactions in solid oxygen, note that the "...softness of the magnon energy spectrum in the β configuration, which causes a higher entropy with respect to the α phase," may be of crucial importance for the α-β phase transition. Their results, however, are based in the spin-wave approximation for classical spins, and a particular structure for the spins in the β phase was assumed.
[48] A. J. R. da Silva and L. M. Falicov, Chem. Phys. Lett. **222**, 339 (1994).
[49] N. F. Mott, *Metal-Insulator Transitions* (Taylor & Francis, London, 1974).
[50] L. M. Falicov, in *Recent Progress in Many-Body Theories*, edited by A. J. Kallio, E. Pajanne, and R. F. Bishop (Plenum, New York, 1988), Vol. 1, p. 275.
[51] P. O. Löwdin, J. Chem. Phys. **18**, 365 (1950).
[52] A. A. Radzig and B. M. Smirnov, *Reference Data on Atoms, Molecules, and Ions* (Springer-Verlag, Berlin, 1985), p. 446.
[53] The value of the phenomenological Heisenberg interaction J used in the present work is defined as twice that used in the work of Stephens and Majkrzak, Ref. 25.
[54] A. J. R. da Silva and L. M. Falicov, in *New Trends in Magnetic Materials and their Applications*, edited by J. L. Morán-López and J. M. Sánchez (Plenum, New York, 1994).
[55] The fact that in the calculated spectra of α and β oxygen the molecular Frenkel excitons are separated in energy from the charge-transfer states is related to the size of the cluster. For the four-molecule cluster the highest-energy molecular exciton can only involve up to four Frenkel excitons, whereas in the solid there will be excitations composed of as many Frenkel excitons as the number of molecules. This would result in the overlap between the many-molecular-exciton states and the charge-transfer band.
[56] C. Kittel, *Quantum Theory of Solids* (Wiley, New York, 1963), Chap. 4.
[57] A. J. R. da Silva, Ph.D. thesis, University of California, Berkeley, 1994.
[58] It should be noted that the total free energy cannot be obtained from the present small-cluster calculation. The lattice contributions to the free energy (both to the internal energy and entropy) are not included in the model. Therefore, the α-β phase transition temperature cannot be predicted. However, the low-energy electronic excitations from the spectra in Figs. 8 and 11 can be used to estimate the magnetic contribution to the entropy. In particular, they can be used to calculate the magnetic entropy difference $\Delta S_{\beta\alpha}(T)$ at the transition temperature, $T = T_{\alpha\beta} = 23.9$ K.
[59] K. D. Bier and H. J. Jodl, J. Chem. Phys. **81**, 1192 (1984).